INVESTIGATION OF THE ANGULAR DEPENDENCE OF THE CROSS SECTION FOR PHOTOPRODUCTION OF CHARGED PIONS ON NUCLEONS

M. I. ADAMOVICH, V. G. LARIONOVA, R. A. LATYPOVA, A. I. LEBEDEV, S. P. KHARLAMOV, and F. R. YAGUDINA

P. N. Lebedev Physics Institute, Academy of Sciences, U.S.S.R.

The differential cross sections for the $\gamma + p \rightarrow n + \pi^+$ process were measured for γ-quantum energies 200, 205 and 210 MeV and meson emission angles 16, 24, 36, 44, 56, 64, 76, 84, 96, 104, 116, 124, 136, 144 and 156° relative to the photon beam in the laboratory system. A phenomenological analysis of the results is carried out and some multipole charged-meson photoproduction amplitudes are determined. The results are compared with the predictions of the dispersion-relation theory.

1. INTRODUCTION

THE determination of multipole photoproduction amplitudes from the experimental data and the construction of photoproduction dynamic models based on the dispersion relations call for an experimental determination of the angular and energy distributions of photo pions with good statistical accuracy.

The photoproduction of π^+ mesons on hydrogen was investigated in many laboratories. Only recently, however, were experimental results obtained on the angular distribution of the pions for photon energies exceeding 230 MeV. In the near-threshold region of photon energies, the experimental data are very skimpy and sketchy.

We have determined in this paper the differential cross sections for the production of π^+ mesons by photons of energy 200, 205, and 210 MeV. We present a phenomenological analysis of these results in conjunction with data on the photoproduction of π^+ and π^- mesons on deuterium, and compare the experimental results with calculations based on the dispersion relations.

2. EXPERIMENT

In the experiment, the pions were produced in a liquid-hydrogen target placed in the bremsstrahlung beam of electrons accelerated to 265 MeV in the FIAN synchrotron. A diagram of the experimental setup is shown in Fig. 1. The setup is separated from the accelerator by lead screens. The photon beam was shaped by two lead collimators. After passing through the second collimator, the photon beam entered an evacuated tube leading to the liquid-hydrogen target. To remove the charged particles from the photon beam, a clearing electromagnet was placed at the entrance to the vacuum duct. The transverse dimensions of the photon beam in the working part of the target were 5.0 × 0.5 cm.

The pions produced in the target emerged through thin aluminum windows and were registered outside the vacuum chamber by stacks of NIKFI BK-400 pellicles. The stacks were secured in such a way that the pions entered the stacks from the end. The working stack was placed between emulsion blocks. The particle loss due to scattering in the stack was compensated by the particles scattered in the emulsion blocks. The pions were registered at 15 emergence angles relative to the direc-
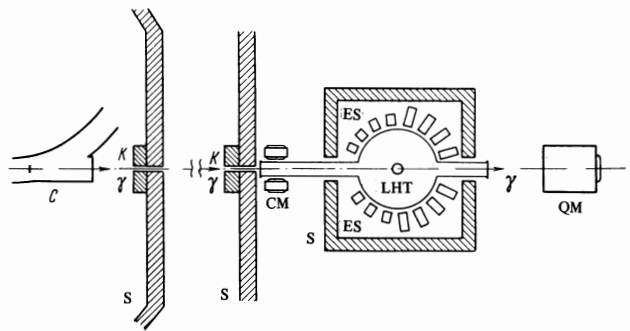

FIG. 1. Diagram of experimental setup. C — Synchrotron chamber, γ — photon beam, K — collimators, CM — clearing magnet, LHT — liquid-hydrogen target, ES — emulsion stacks recording the pions, QM — quantum meter, S — shield.

tion of the photons. The total energy flux of the photon beam was registered by a quantum meter placed behind the vacuum chamber. After irradiation, the stacks were marked by collimated x-radiation in the RUP-200 setup. The marked stacks were separated into individual pellicles, which were then mounted on glass and developed in the usual manner.

The emulsions were scanned with MBI-1 and MBI-2 microscopes at a magnification 20 × 7 × 1.5. The registration efficiency was 99%. It was verified by sample scanning of the emulsions by different observers. All π-μ decays were registered and, for additional control, also the muon and pion tracks near the possible stopping place. In the course of processing, the π and μ meson tracks were traced in neighboring layers, making it possible to identify reliably the π-μ decays, to eliminate the random background of π^+ mesons, and to monitor the scanning the neighboring pellicles.

The π^+ background from the target walls was 0.9%. It was determined from the number of registered negative pions and the known σ^-/σ^+ ratio for heavy nuclei. For each of the observed pions, we determined the kinetic energy from the residual range in the emulsion. In determining the pion energy, we took into account the energy loss in liquid hydrogen, in the target walls, in the aluminum windows of the chamber, and in the stack holder.

Table I. Differential cross sections for the photoproduction
of positive pions on hydrogen in the c.m.s. at photon
energies 200, 205, and 210 MeV.
The cross sections are given in units of 10^{30} cm^2/sr.

θ_{cms}, deg	E_γ, MeV (lab)								
	200			205			210		
	$\frac{d\sigma}{d\Omega}$	δ, %	Δ, %	$\frac{d\sigma}{d\Omega}$	δ, %	Δ, %	$\frac{d\sigma}{d\Omega}$	δ, %	Δ, %
21	7.86	5.8	8.0	7.29	6.3	8.4	6.13	7.4	9.2
31	7.70	7.6	9.4	7.09	8.3	10.0	7.08	8.6	10.2
46	8.01	5.8	8.0	8.16	5.9	8.1	6.32	7.2	9.0
56	7.79	5.1	7.5	8.75	5.1	7.5	8.46	5.4	7.7
70	8.62	5.7	7.9	8.77	5.9	8.0	9.13	6.0	8.1
79	9.07	5.0	7.4	9.73	5.0	7.5	11.12	4.9	7.3
92	10.06	4.0	6.8	10.58	4.0	6.8	11.07	4.1	6.8
101	9.00	20.2	20.9	9.39	20.2	20.9	9.94	20.2	20.9
111.5	9.38	5.4	7.7	10.42	5.3	7.6	11.31	5.2	7.6
119.5	12.05	6.9	8.8	11.82	7.1	9.0	13.50	6.8	8.7
131	11.03	7.3	9.2	9.99	7.3	9.1	11.28	7.2	9.0
137.5	11.00	5.7	7.9	10.19	6.1	8.2	12.93	5.5	7.8
147	10.46	4.3	7.0	10.63	4.3	7.0	10.55	4.4	7.0
151.5	11.73	12.8	13.9	9.26	14.6	15.6	13.57	12.2	13.4
162.5	10.98	6.4	8.4	9.68	6.9	8.8	9.86	6.9	8.8

3. EXPERIMENTAL DATA

The measured yields were used to calculate the pion
photoproduction cross sections in the intervals
197.5—202.5, 202.5—207.5, and 207.5—212.5 MeV. In
each energy interval, the pion yield $C(\theta)$ at a definite
angle θ_{lab} is connected with the average pion photo-
production differential cross section $d\sigma/d\Omega(\theta)$ in the
following manner:

$$C(\theta) = \eta \frac{d\sigma}{d\Omega_{lab}}(\theta) N_H \frac{W_0}{E_0} \frac{B(k_0)}{k_0} \Delta k R_{\pi\mu} A_\pi l \Delta\Omega_{lab}, \quad (1)$$

where N_H is the number of hydrogen nuclei per cm^2,
$(W_0/E_0)(B(k_0)/k_0)\Delta k$ the number of photons with energy
k_0 in the interval Δk of the bremsstrahlung spectrum of
the electrons with energy E_0, W_0 the total energy of the
photon beam, $\Delta\Omega$ the solid angle, l the effective target
thickness, η the scanning efficiency, $R_{\pi\mu}$ the correction
factor for pion knock-out from the beam by π-μ decays
in flight, and A_π a correction factor for the knock-out of
pions from the beam as a result of interaction with the
matter.

The obtained c.m.s. differential cross sections and
their errors are listed in Table I. The errors can be
divided into two classes. The first includes errors that
depend on the pion energy and therefore differ for dif-
ferent pion emission angles. These include also errors
due to the inaccuracy of the correction factors $R_{\pi\mu}$ and
A_π. The total error due to the correction factors ranges
from 0.1 to 3%, depending on the energy. The total er-
rors due to the statistics and the first-class errors are
designated by δ in Table I.

The second class of errors includes those that do not
depend on the energy and are therefore constant for

Table II. Uncertainties in the quantities used to
calculate the cross sections.

Quantity	Error, %
Number of hydrogen nuclei N_H.	1
Ionization curve measured by the quantum meter	1
Maximum photon energy E_0	2
Uncertainty in the form of the bremsstrahlung spectrum	2
Photon energy interval Δk	2
Solid angle $\Delta\Omega$	3
Summary rms error	4,8

different pion angles and energies. These errors are
summarized in Table II. The error in the calibration of
the quantum meter is 3%.

Table I lists also the total error Δ of the differential
cross section, which includes, besides δ, the errors
indicated in Table II. The data of Table I are plotted in
Figs. 2—4, which show the angular distributions of the
pions produced by photons with energies 200, 205, and
210 MeV.

4. APPROXIMATION OF THE ANGULAR DEPENDENCE OF THE DIFFERENTIAL CROSS SECTION

According to the phenomenological theory, the angu-
lar dependence of the cross section for photopion pro-
duction can be approximated by polynomials in powers
of cos θ:

$$\frac{d\sigma}{d\Omega}(\theta) = \sum_{j=0}^{j=k} a_j \cos^j \theta, \quad (2)$$

where θ is the c.m.s. angle between the directions of
the photon motion and of the emerging pion.

However, allowance for the term describing the
direct interaction between the photon and the meson
current makes it necessary to use in the analysis of the
angular dependence of the charged pions an approxima-
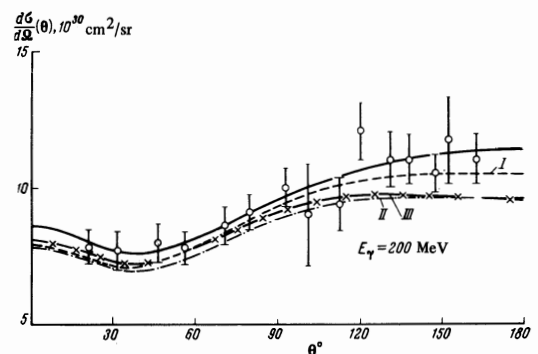tion of the form

FIG. 2. Angular distribution of π^+ mesons produced by photons with
energy 200 MeV. Solid curve — approximation of experimental data,
curve I — approximation I, curve II — approximation II, curve III — ap-
proximation III.

$$(1 - \beta \cos \theta)^2 \frac{d\sigma}{d\Omega}(\theta) = \sum_{n=0}^{m-1} A_n \cos^n \theta, \qquad (3)$$

where β is the pion velocity in the c.m.s. The coefficients A_n were determined during the course of processing the obtained cross sections $d\sigma/d\Omega(\theta)$ with an M-20 electronic computer, by determining the minimum of the functional

$$M = \sum_{i=1}^{N} \left[(1 - \beta \cos \theta_i)^2 \frac{d\sigma}{d\Omega}(\theta_i) - \sum_{n=0}^{m-1} A_n \cos^n \theta_i \right]^2. \qquad (4)$$

The summation is over all the experimental values of θ_i, m is the number of free parameters, and $N - m$ is the number of degrees of freedom.

The coefficients a_j were calculated in similar fashion. Table III lists the values of the coefficients a_j, χ_0^2 and $\chi_0^2/(N - m)$ and of the probability $\mathscr{P}(\chi^2 > \chi_0^2)$ for the angular distribution of the pions at a photon energy 200 MeV. From the χ^2 criterion, and also from the error of the last coefficient, it follows that the best description of the angular distribution is obtained by a binomial of the type $a_0 + a_1 \cos \theta$. This is evidence of preferred production of pions in the S state and of the presence of interference between the S and P states.

Table IV lists the values of the coefficients A_n together with χ_0^2, $\chi_0^2/(N - m)$, and the probability $\mathscr{P}(\chi^2 > \chi_0^2)$. Comparison of $\chi_0^2/(N - m)$ and $\mathscr{P}(\chi^2 > \chi_0^2)$ from this table with the corresponding values from Table III shows that the approximation (3), in which the delay term is taken into account is preferrable to the approximation (2). This demonstrates the need for taking into account the contribution of the direct interaction between the photons and the pion current at a γ-quantum energy 200 MeV.

The best description of the experimental data in the form (3) is given by the trinomial

$$F(\cos \theta) = (1 - \beta \cos \theta)^2 \frac{d\sigma}{d\Omega}(\theta) = A_0 + A_1 \cos \theta + A_2 \cos^2 \theta. \quad (5)$$

Extrapolation of the function $F(\cos \theta)$ to the pole $\cos \theta = 1/\beta$ makes it possible to estimate the constant of the pion-nucleon interaction f^2 by means of the formula

$$F\left(\frac{1}{\beta}\right) = \alpha \lambda^2 f^2 \frac{q}{k^3} \frac{1 - \beta^2}{(1 + \omega/M)^2}, \qquad (6)$$

where $\omega = \sqrt{1 + q^2}$, q is the pion momentum, k is the photon momentum, M is the nucleon mass, $\alpha = 1/137$ and λ is the Compton wavelength of the pion. The ob-
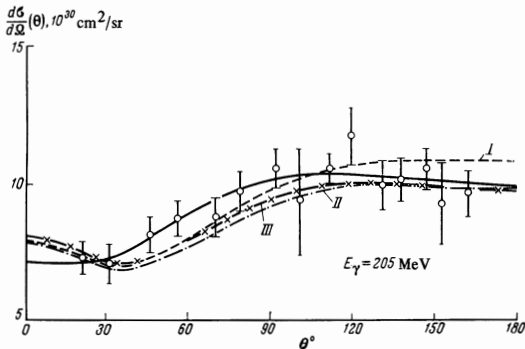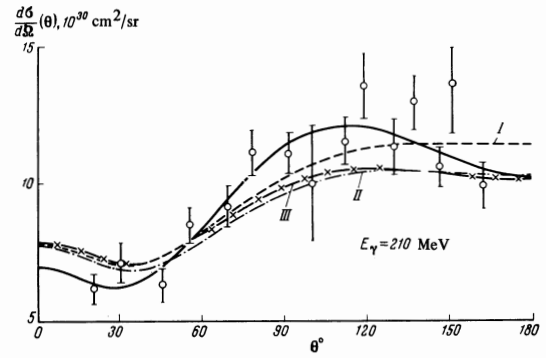

FIG. 4. Angular distribution of π^+ mesons produced by photons with energy 210 MeV. The symbols are the same as in Figs. 2 and 3.

tained value of the pion-nucleon coupling constant is $f^2 = 0.07 \pm 0.02$. The low accuracy of this determination is due to the large extrapolation interval and the lack of the data closest to the pole directly at the angle $\theta = 0°$. At the same time, if we use as additional experimental information the value $f^2 = 0.08 \pm 0.003$, which is known from scattering measurements, and the value of the differential cross section at the pole corresponding to this constant, then we can attempt to determine again the law governing the angular distributions. The best sets of the coefficients A_n determined in this manner for photon energies 200, 205, and 210 MeV are listed in Table V.

By way of an example, we present below also the error matrix of the coefficients A_n for 200 MeV energy:

$$\begin{pmatrix} 0.051 & -0.083 & 0.031 \\ & 0.178 & -0.078 \\ & & 0.037 \end{pmatrix} \cdot 0.656.$$

As seen from Table V, when $E_\gamma = 200$ MeV the best approximation

$$F(\cos \theta) = (1 - \beta \cos \theta)^2 \frac{d\sigma}{d\Omega}(\theta)$$

is attained by means of a trinomial, whereas a description of the angular distributions at higher photon energies already calls for polynomials with four terms. This is evidence of the greater contribution of the P-wave pion production on going to higher energies.

The best approximations of the angular distributions of the pions at photon energies 200, 205, and 210 MeV are shown in Figs. 2—4 by solid lines.

5. APPROXIMATION OF THE ANGULAR DEPENDENCE OF THE RATIO σ^-/σ^+

Figure 5 shows the angular dependence of the ratio σ^-/σ^+ for $E_\gamma = 200$ MeV. The yields of the negative and positive pions on deuterium were measured by Sands et al.[1], Beneventano et al.[2], Walker and Burq[3], Rutherglen and Walker[4], and Bazin and Pine[5]. These data were analyzed with allowance for the corrections for the Coulomb and nuclear interactions in accordance with the work of Baldin[6] and Bazin and Pine[5], and also with allowance for the corrections for the difference in the photoproduction thresholds of pions having different signs[7]. The values of σ^-/σ^+ for nucleons, together with the pole value

$$\frac{\sigma^-}{\sigma^+}\left(\arccos\frac{1}{\beta}\right) = \frac{(1 - \beta\cos\theta)^2 d\sigma^-/d\Omega}{(1 - \beta\cos\theta)^2 d\sigma^+/d\Omega}\bigg|_{\cos\theta=1/\beta} = 1.00 \pm 0.05, \quad (7)$$

FIG. 3. Angular distribution of π^+ mesons produced by photons with energy 205 MeV. The symbols are the same as in Fig. 2.

Table III. Values of the coefficients a_j obtained in approximating the angular dependence by means of polynomials

$$\sum_{j=0}^{k} a_j \cos^j \theta.$$

a_0	a_1	a_2	a_3	χ_0^2	$\dfrac{\chi_0^2}{N-m}$	$\mathscr{P}(\chi^2 > \chi_0^2)$
9.4±0.20	−1.9±0.31			6.526	0.543	0.885
9.4±0.26	−1.9±0.24	−0.06±0.50		6.518	0.593	0.835
9.4±0.26	−2.7±0.69	−0.2 ±0.50	1.2±1.0	5.659	0.566	0.845

Table IV. Values of the coefficients a_n, obtained by using the approximation

$$(1 - \beta \cos \theta)^2 \frac{d\sigma}{d\Omega}(\theta) = \sum_{n}^{m-1} A_n \cos^n \theta$$

A_0	A_1	A_2	A_3	A_4	χ_0^2	$\dfrac{\chi_0^2}{N-m}$	$\mathscr{P}(\chi^2 > \chi_0^2)$
9.5±0.17	−13.8±0.34	5.6±0.36			5.511	0.459	0.937
9.5±0.26	−13.9±0.53	5.6±0.66	0.6±0.81		5.509	0.508	0.928
9.5±0.28	−14.1±0.92	6.0±1.43	0.4±1.46	−0.6±1.46	5.453	0.545	0.857

Table V. Values of the coefficients A_n, obtained by approximating the angular distributions of the photopions with allowance for the value of $F(\cos \theta)$ at the pole.

| E_γ, MeV	A_0	A_1	A_2	A_3	A_4	χ_0^2	$\dfrac{\chi_0^2}{N-m}$	$\mathscr{P}(\chi^2 > \chi_0^2)$
200	9.5±0.15	−13.9±0.28	5.8±0.13			5.60	0.431	0.958
205	10.1±0.19	−13.9±0.27	3.6±0.46	1.3±0.23		4.69	0.391	0.966
210	11.3±0.46	−18.3±1.20	4.8±0.84	5.1±1.85	−1.9±0.91	13.72	1.248	0.250

calculated using the known quantity $f^2 = 0.08 \pm 0.003$, were approximated by polynomials in powers of $\cos \theta$. The best description of the angular dependence shown in Fig. 5 is the polynomial:

$$\sigma^-/\sigma^+ = (1.31 \pm 0.018) - (0.19 \pm 0.026)\cos\theta \qquad (8)$$

with $\chi_0^2 = 16.62$, $\chi_0^2/(N - m) = 1.512$, and a probability $\mathscr{P}(\chi^2 > \chi_0^2) = 0.120$. The error matrix for this polynomial is

$$\begin{pmatrix} 0.000295 & 0.000018 \\ & 0.000557 \end{pmatrix} \cdot 1.51.$$

The obtained dependence of σ^-/σ^+ on $\cos \theta$ agrees with the notion of preferred formation of pions in the S state in the near-threshold region of the photon energies.
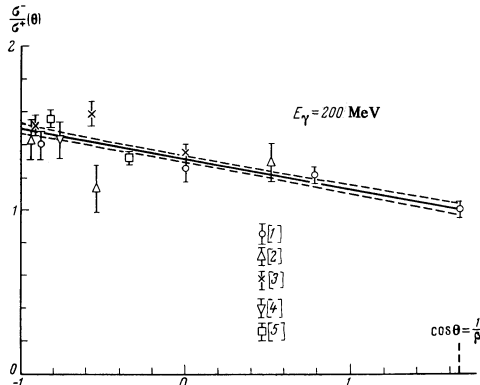
FIG. 5. Angular distribution of the ratio σ^-/σ^+ for photons with energy 200 MeV.

6. PHENOMENOLOGICAL ANALYSIS OF THE DATA

Using the values of the empirical coefficients A_n (Table V), we have extrapolated the differential cross sections for the photoproduction of π^+ mesons to 0 and 180°. We similarly extrapolated the ratio σ^-/σ^+ to 0 and 180°. The differential cross sections $d\sigma^-/d\Omega$ for the photoproduction of negative pions on neutrons at 0 and 180° were obtained by multiplying $d\sigma^+/d\Omega$ by σ^-/σ^+, taken at the corresponding angles. Table VI lists the values of $(k/q)d\sigma^+/d\Omega$ and $(k/q)d\sigma^-/d\Omega$ at $\theta = 0$ and 180° for $E_\gamma = 200$ MeV.

In the near-threshold photon energy region, where $q^2 < 1$ (in our case $q^2 \leq 0.57$), the square of the photoproduction matrix element is connected with the multipole amplitudes $E_{l\pm}$ and $M_{l\pm}$ ($l_\pm$ denotes the total angular momentum $j = l \pm 1/2$) in the following manner:

$$\frac{k}{q}\frac{d\sigma}{d\Omega}\binom{0°}{180°} = [E_{0+} \pm (M_{1+} - M_{1-} + 3E_{1+})]^2 = (E_{0+} \pm \Delta)^2. \qquad (9)$$

These expressions were obtained under the following assumptions: 1) the imaginary parts of the multipole amplitudes are negligibly small; 2) the pions are produced in S and P states.

The first assumption is correct because the pion-nucleon scattering phases are small. The second assumption is confirmed by all the known data on the near-threshold pion photoproduction, including the results described in the two preceding sections. In addition, we used the impulse approximation in describing the photoproduction of the charged pions on deuterium.

Table VI.

θ	$0°$	$180°$
$\dfrac{k}{q}\dfrac{d\sigma^+}{d\Omega}(\theta)$	13.7 ± 0.80	18.0 ± 0.50
$\dfrac{k}{q}\dfrac{d\sigma^-}{d\Omega}(\theta)$	15.3 ± 0.97	27.0 ± 0.88

The amplitudes for the photoproduction of π^+ and π^- mesons are related by the equations

$$F(\pi^+)=\sqrt{2}(F^{(0)}+F^{(-)}),\quad F(\pi^-)=\sqrt{2}(F^{(0)}-F^{(-)}),\qquad (10)$$

where $F^{(0)}$ is the isoscalar amplitude and $F^{(-)}$ the isovector amplitude.

From formulas (9) and (10) and from Table VI we obtain the amplitudes E_{0+} and Δ as well as their isotopic components for the photoproduction of pions by 200-MeV γ quanta. They are listed in Table VII.

Generally speaking, we should have obtained four solutions for the amplitudes. However, the requirement that the sign of the resonant P-wave amplitude and the signs in the coefficients A_1 for the angular distribution of the pions be positive leads to the choice of signs indicated in Table VII.

7. ANALYSIS OF DATA ON THE BASIS OF THE THEORY OF DISPERSION RELATIONS

The dispersion relations for the amplitudes of photoproduction near threshold have the following structure:

$$F^{(-)}=P^{(-)}+I^{(-)}(3/2,\,3/2)+I^{(-)}(1/2,\,3/2)+I^{(-)}(S,P),$$
$$F^{(0)}=P^{(0)}+I^{(0)}(S,P)+P_\rho,\qquad (11)$$

where P is the pole (Born) term, which is proportional to αf, I are the dispersion integrals of the imaginary parts of the amplitudes, and P_ρ is the contribution of the resonant pion-pion interaction (ρ-meson) to the isoscalar amplitude.

The explicit form of the dispersion relations was obtained in[8]. Neglecting the contributions of the dispersion integrals, we obtained the so-called pole approximation, which is the governing approximation for charged pions. Usually in the calculation of dispersion integrals one usually takes account of the contribution made to them only by the imaginary part of the resonant amplitude $M_{1+}^{3/2}$ (the so called resonance approximation). However, as indicated in[9], the imaginary part of the pion photoproduction amplitude in the second resonant state may make a noticeable contribution to the dispersion integrals. Appreciable interest attaches also to an estimate of the contribution made to the dispersion

integrals by the imaginary parts of the nonresonant S- and P-wave amplitudes.

The contribution to the dispersion integrals from the nonresonant amplitudes I(S, P) and from the amplitude of the second resonant state I(1/2, 3/2), as well as an estimate of the uncertainty in the calculation of the integral I(3/2, 3/2), due to the imaginary part of the amplitude for the photoproduction of the pions in the first resonant state of the π-N system, were all calculated earlier[9]. We present below a comparison of the results of calculations made in accordance with different models with the experimental cross sections and amplitudes.

The curves marked I in Figs. 2, 3, and 4 represent the angular distributions calculated from the dispersion relations with account taken of only the imaginary part of the resonant amplitude $M_{1+}^{3/2}$ in the dispersion relations (we shall call these calculations approximation I). As seen from the figures, a qualitative agreement is observed between the results of such calculations and experiment. Allowance for the second resonance in the dispersion relation (approximation II) leads to results that deviate appreciably from the experimental cross sections (curves II on Figs. 2, 3, and 4). The influence of the dispersion integrals of the imaginary parts of the S-wave amplitudes and small P-wave amplitudes, which are taken into account in approximation III, can be assessed from the difference between curves III (which were calculated in this approximation) and the curves II. As seen from these estimates, their influence on the cross sections is relatively small.

Thus, allowance for the amplitude of the second resonance and for the nonresonant S- and P-wave photoproduction amplitudes in the dispersion integrals leads to an increase in the disparity between the theoretically calculated and experimental values of the differential cross sections of π^+-meson photoproduction on protons.

We now compare the calculations obtained in Sec. 6 for E_γ = 200 MeV with the experimental values of the amplitudes E_{0+} and Δ. In Table VII we list, together with the experimental values, the results of calculations made in the different approximations.

It should be noted first that all the amplitudes, with the exception of $\Delta(\pi^\pm)$ and $\Delta^{(-)}$, are governed almost entirely by the contribution of the pole term. The contribution of the first resonance I(3/2, 3/2) to the amplitudes $E_{0+}(p^\pm)$ and $E_{0+}^{(-)}$ is insignificant. By virtue of its isovector nature, it makes no contribution to the isoscalar amplitudes $E_{0+}^{(0)}$ and $\Delta^{(0)}$. A significant contribution is made by the first resonance to the combination of the P-wave amplitudes $\Delta^{(-)}$. It should be noted that in approximation I the amplitudes $E_{0+}^{(0)}$, $\Delta(\pi^\pm)$, $\Delta^{(-)}$, and

Table VII.

	$E_{0+}(\pi^+)$	$-E_{0+}(\pi^-)$	$E_{0+}^{(-)}$	$-E_{0+}^{(0)}$	$-\Delta(\pi^+)$	$\Delta(\pi^-)$	$-\Delta^{(-)}$	$\Delta^{(0)}$
Experiment	$3.97\pm$ ±0.06	$4.55\pm$ ±0.075	$3.01\pm$ ±0.034	$0.205\pm$ ±0.034	$0.27\pm$ ±0.06	$0.64\pm$ ±0.075	$0.32\pm$ ±0.034	$0.13\pm$ ±0.034
Pole (Born) approximation	3.771	4.394	2.887	0.220	-0.173	0.224	0.018	0.141
Approximation I	3.792	4.415	2.902	0.220	0.268	0.666	0.330	0.141
Approximation II	3.692	4.316	2.831	0.220	0.183	0.580	0.270	0.140
Approximation III	3.720	4.456	2.891	0.260	0.148	0.546	0.245	0.141

$\Delta^{(0)}$ agree with experiment within the limits of the standard errors indicated in the table. No such agreement is observed for the amplitudes $E_{0+}(\pi^{\pm})$ and $E_{0+}^{(-)}$. The values of the isovector amplitudes, calculated with the amplitude of the second resonance taken into account in the dispersion relations (approximation II), is in poor agreement with the experimental values.

The contribution of the imaginary parts of the non-resonant S- and P-wave amplitudes to the dispersion integrals (approximation III) practically compensates the contribution of the second resonance to the S-wave amplitude $E_{0+}^{(-)}$, but increases still further the disparity with experiment for the isovector combination of the P-wave amplitudes $\Delta^{(-)}$. In this approximation, the agreement with experiment is also worse for the isoscalar S-wave amplitude $E_{0+}^{(0)}$. Thus, the theoretical estimates and the approximations under consideration do not describe with sufficient accuracy the experimental values of the isotopic photoproduction amplitudes.

As seen from the table, the isoscalar combination of P-wave amplitudes $\Delta^{(0)}$ is determined only by the pole term. Therefore the amplitude $\Delta^{(0)}$ is best used for an estimate of the contribution of the $\gamma\pi\rho$ interaction. Preliminary estimates of this contribution from the entire aggregate of the results on the photoproduction of charged pions in the energy interval 165—200 MeV were published earlier [10].

The small values of the considered dispersion integrals in the amplitudes $E_{0+}(\pi^+)$ and $E_{0+}^{(-)}$ give grounds for hoping that a comparison of the theoretical values of the amplitudes, calculated in this manner, with their experimental values can yield sufficiently accurate information on the πN-interaction constant f^2. From the value of the amplitude $E_{0+}^{(-)}$ for $E_\gamma = 200$ MeV, listed in the Table VII, we get, when account is taken of the error in the absolute calibration of the photon beam, $f^2 = 0.087 \pm 0.003$.

If we neglect in the amplitude $\Delta^{(0)}$ the possible contribution of the $\gamma\pi\rho$ interaction, then we get from a comparison of the experimental and theoretical values of this amplitude $f^2 = 0.07 \pm 0.036$, which agrees with the result obtained by extrapolating the expression to the pole $\cos\theta = 1/\beta$.

$$F^{(\pi+)}(\theta) = (1 - \beta\cos\theta)^2 \frac{d\sigma^{(\pi+)}}{d\Omega}(\theta).$$

The observed discrepancy between the photoproduction amplitudes calculated from the one-dimensional dispersion relations and those obtained by experiment can also be due to insufficient knowledge of the imaginary parts of the photoproduction amplitudes used in the calculation of the dispersion integrals. Therefore, to obtain more accurate values of the constants of the πN coupling and of the $\gamma\pi\rho$ interaction it is necessary, besides refining the data on the photoproduction of the pions at energies near threshold, to investigate further the photoproduction in the high-energy region.

[1] M. Sands, J. G. Teasdale, and R. L. Walker, Phys. Rev. 95, 592 (1954).

[2] M. Beneventano, G. Bernardini, G. Stoppini, and L. Tau, Nuov. Cimento 10, 1109 (1958).

[3] J. K. Walker and J. P. Burq, Phys. Rev. 132, 447 (1963).

[4] J. G. Rutherglen and J. K. Walker, Proc. Phys. Soc. 76, 430 (1960).

[5] M. I. Bazin and J. Pine, Phys. Rev. 132, 2735 (1963).

[6] A. M. Baldin, Trudy, Physics Institute, Academy of Sciences, SSSR 19, 3 (1963); Nuovo Cimento 8, 569 (1958).

[7] S. P. Kharlamov, M. I. Adamovich, and V. G. Lapionova, Zh. Eksp. Teor. Fiz. 36, 945 (1959) [Sov. Phys.-JETP 9, 668 (1959)].

[8] A. A. Logunov, A. N. Tavkhelidze, and L. D. Solov'ev, Nucl. Phys. 4, 427 (1957); G. F. Chew, M. L. Goldberger, F. E. Low, and Y. Nambu, Phys. Rev. 106, 1345 (1957).

[9] M. I. Adanovich, V. G. Larionova, A. I. Lebedev, S. P. Kharlamov, and F. R. Yagudina, Trudy, Physics Institute, Academy of Sciences SSSR 34, 57 (1966).

[10] M. I. Adamovich, V. G. Larionova, A. I. Lebedev, S. P. Kharlamov, and F. R. Yagudina, ZhETF Pis. Red. 2, 490 (1965) [JETP Lett. 2, 305 (1965)].